

# Electrical conductance of atomic contacts in liquid environments

L. Grüter, M.T. González, R. Huber, M. Calame,\* and C. Schönberger  
*Institut für Physik, Universität Basel, Klingelbergstr. 82, CH-4056 Basel, Switzerland*  
 (Dated: June 20, 2018)

We present measurements of the electrical conductance  $G$  at room temperature of mechanically controllable break junctions (MCBJ) fabricated from Au in different solvents (octane, DCM, DMSO, and toluene) and compare with measurements in air and vacuum. In the high conductance regime  $G \gtrsim G_0 = 2e^2/h$ , the environment plays a minor role, as proven by the measured conductance histograms, which do not depend on the environment. In contrast, the environment significantly affects the electrical properties in the low conductance (tunneling) regime  $G \ll G_0$ . Here, we observe a systematic and reproducible lowering of the tunneling barrier height  $\phi$ . At shorter distances, a transition to a strongly suppressed apparent barrier height is observed in octane, providing evidence for the layering of solvent molecules at small inter-electrodes separations. The presented experimental configuration offers interesting perspectives for the electrical characterization of single molecules in a controlled environment.

The perspectives to develop molecular devices based on single molecule functionalities has recently attracted much attention [1, 2]. Break junctions [3, 4, 5] experiments in vacuum demonstrated that this technique is particularly suited to study the electronic properties of single molecules [6, 7, 8, 9]. Adding a chemically controllable environment in break junctions experiments would offer a variety of interesting possibilities. The electronic properties of a molecule can be tuned for instance by adjusting its redox state using a liquid gate. A liquid environment offers also a better control on the anchoring of the molecule to the metallic constriction. The excellent efficiency of a liquid gate has been demonstrated previously on carbon nanotube field-effect transistors [10], while this effect has been recently studied for organic molecules using a Scanning Tunneling Microscope (STM) [11].

In this letter, we present a break junction setup with an integrated liquid cell, allowing to explore the influence of solvents on the electronic properties of atomic contacts. The setup is used to study the variation of the electrical conductance  $G$  of Au junctions with their elongation in the regime of tunneling (low conductance) and true metallic contact (high conductance). As solvents, we have used deionized water, dichloromethane (DCM), dimethylsulfoxide (DMSO), octane and toluene. The last four are of particular interest since they are potential organic solvents for molecules relevant in molecular electronics. In addition, these solvent cover a broad range of polarities. We also compare the results with reference measurements obtained in vacuum and air.

The suspended metallic bridges were fabricated following a method similar to the one described in Ref. [4]. We use  $0.3 \times 10 \times 24 \text{ mm}^3$  polished phosphor bronze substrates, spin-coated with a 2-3  $\mu\text{m}$  thick polyimide layer (PI2610, HD MicroSystems), and annealed for 30 min at 200 °C in air, and 1 h at 400 °C and in vacuum at

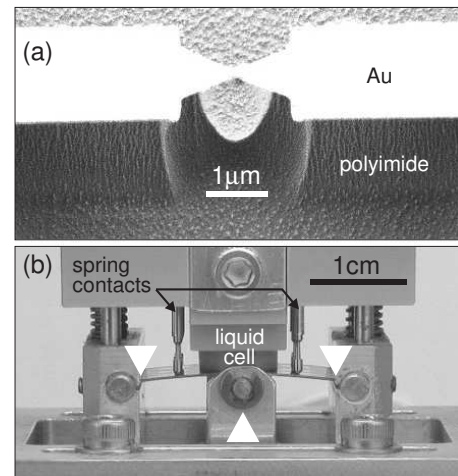


FIG. 1: (a) SEM image of one underetched Au junction defined by electron beam lithography. (b) View of the substrate mounted in the three point bending mechanism (white triangles) with a liquid cell pressed against the substrate.

$10^{-7}$  mbar. The metallic electrodes were produced with a combination of UV and electron beam lithography, followed by a Au-metallization step and an underetching of the junctions using an oxygen plasma (80%  $\text{O}_2$  and 20%  $\text{CHF}_3$ ; 0.1 Torr; 100 W). On a substrate, three junctions with a central constriction 80–150 nm wide (Fig. 1(a)) are fabricated in parallel. The resistance of the junctions ranges typically between 200  $\Omega$  and 300  $\Omega$  for 70 nm thick bridges. The sample is mounted (unclamped) in the three-point-bending mechanism shown in Fig. 1(b). The distance between the counter-supports is 20 mm. The vertical displacement of the pushing-rod pressing on the sample from below is driven by a stepper motor via a coupling gear, allowing for displacement amplitudes up to a few millimeters with a resolution of 3 nm. To perform measurements in a liquid, we integrated a liquid cell formed by a portion of a *Viton*<sup>®</sup> tube, enclosing a volume of 250  $\mu\text{l}$ . The cell includes an inlet and outlet port allowing the exchange of fluids in the course of the

\*Electronic address: michel.calame@unibas.ch

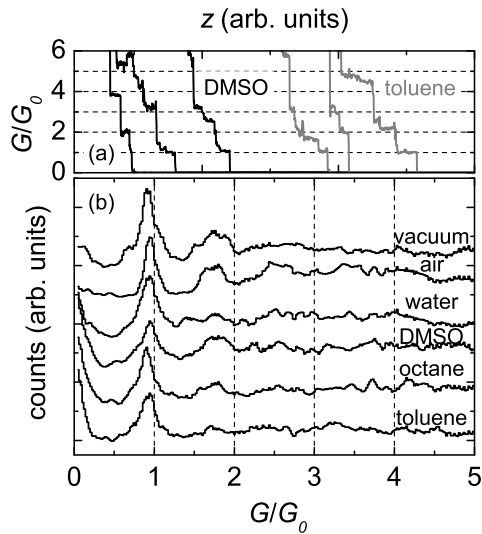


FIG. 2: High conductance regime: (a) Electrical conductance  $G$  scaled to  $G_0 = 2e^2/h$  versus vertical displacement of the push-rod  $z$ , shifted horizontally for clarity, for one gold junction in DMSO and in toluene. (b) Conductance histograms, collected from many measurements of  $G(z)$  of three junctions measured in different environments. The data for DMSO, octane and toluene correspond to one junction, those for air and water to a second one and those for vacuum to a third one. The histograms are shifted vertically for clarity.

measurements. A tight contact of the cell to the sample surface is ensured via a spring. The electrical measurements were performed in a two-probe configuration, using spring-loaded metallic tips. A standard data acquisition board (National Instruments) was used both to apply a constant bias voltage of 0.1 V, and to record the current in the junction as measured by a current-voltage converter.

In the high conductance regime ( $G \gtrsim G_0 = 2e^2/h$ ), for each environment, we collected 100 – 130 curves of the decrease of the junction conductance as a function of the vertical displacement  $z$  of the pushing-rod while extending and, eventually, breaking the constriction. Typical single conductance curves are shown in Fig. 2(a), whereas Fig. 2(b) displays the conductance histogram over all measured curves. In agreement with previous work in air, vacuum and at low temperatures (He), there are large junction-to-junction variations in  $G(z)$ . Individual curves display plateaux at different conductance values. The clearest and most reproducible plateau is the one close to  $1 G_0$ , as expected for monovalent wires [13], and gives rise to a clear peak in the histograms shown in Figure 2(b). Each histogram is built from all the conductance traces measured in one environment (bin width:  $0.02 G_0$ ) and normalized by the total number of counts. Because no striking difference between histograms for different environments are apparent, we conclude that the environment plays a minor role in the electronic proper-

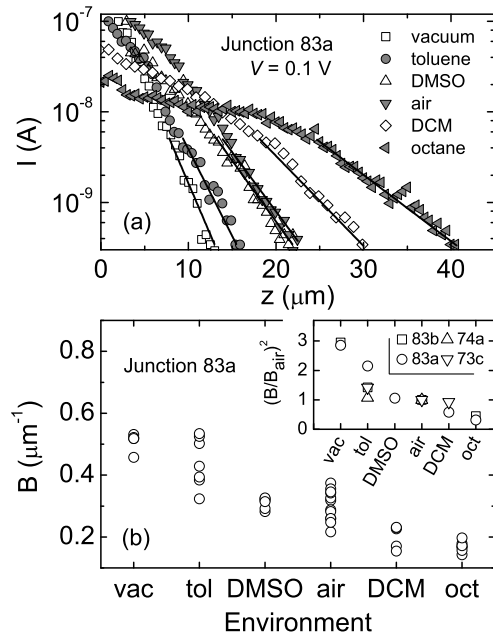


FIG. 3: Tunneling regime: (a) Raw data for the electrical current  $I$  versus vertical displacement of the push-rod  $z$  for a single gold junction (83a) in different environments. The curves are shifted horizontally for clarity, and the zero in  $z$  has been arbitrarily chosen. The solid lines are obtained from fits of  $I$  to an exponential law, i.e.  $\ln(I) = -BI + const.$  (b) Results for the slope  $B$  from fitting an exponential law to several sets of curves similar to that shown in part (a). The ratio of the mean value of  $B$  in different environments with respect to that of air has been plotted in the inset for four different junctions.

ties of atomic contacts in the *high* conductance regime.

We now focus on the behavior of the junctions in the tunneling regime ( $G$  between  $4 \times 10^{-5}$  and  $0.01 G_0 = 2e^2/h$ ). Several sets of 10 consecutive open-close cycles (up to a conductance of a few  $G_0$ ) were recorded for the same junction in different environments. Fig. 3(a) shows representative raw curves obtained when the junction was being closed. In the low current regime ( $\leq 5 \times 10^{-9}$  A), subsequent curves show little variation, and exhibit a well defined linear regime in a semi-log representation. At higher currents, we observed larger curve-to-curve variations that can be attributed to differences in the microscopic configurations of the junctions. Whenever measuring in a medium different from vacuum, a clear decrease of the slope at low currents is observed which is characteristic for each environment. We emphasize that the slope is not correlated with the order in which the environments were tested and, hence, with a possible accumulation of contamination in the junction.

We consider the simple expression for the tunneling current at low bias voltage through a square barrier of

height  $\phi$  and thickness  $d$ ,  $I \propto \exp[-2d\sqrt{2m\phi}/\hbar]$ , where  $m$  is the electron mass and  $d = r(z - z_0)$  the distance between the two extremities of the Au contacts on either side. Here,  $r$  is the mechanical reduction factor, which can be obtained from the geometry of the junction [5, 12] and  $z_0$  is a constant. We then have  $\ln(I) = -Bz + \text{const}$ , where  $B = 2r\sqrt{2m\phi}/\hbar = 1.025[\text{eV}^{-0.5}\text{\AA}^{-1}]\sqrt{\phi}r$ . Hence, the slope of  $\ln(I)$  vs  $-z$  is given by  $B \propto \sqrt{\phi}$ . A large (small) slope corresponds to a large (small) barrier height  $\phi$ . To reduce the effect of fluctuations, the slope  $B$  was deduced in the low current regime using all 10 curves of each set of measurements simultaneously. The result of several sets is shown in Fig. 3(b) for the same junction as in Fig. 3(a). The lines in Fig. 3(a) correspond to the averaged values of  $B$  for each environment.

We performed the same analysis for three additional samples and found differences up to a factor of 3 in  $B$  for a given environment. This large scattering cannot be assigned to  $\phi$ , because unphysically large barrier heights would then result. The scattering is due to sample-to-sample variation in the mechanical reduction factor  $r$ . This is proven with the inset of Fig. 3(b) which illustrates the ratio  $(B/B_{\text{air}})^2$  for each environment and for four different junctions. This ratio is directly proportional to the ratio of the effective barrier heights and does *not* depend on  $r$ . We conclude, that  $\phi$  does depend on the environment in a specific and reproducible way.

Reduced effective tunneling barrier heights  $\phi$  have been consistently observed in STM experiments performed in aqueous environments [14, 15, 16]. Although a detailed model providing a quantitative account for this decrease is still lacking, we point out that the observed decrease in  $\phi$  does not show a simple correlation with the dielectric constant (whether static or optical) of the medium in between the electrodes [17, 18].

As we have stressed before, the mechanical reduction factor  $r$  presents a large uncertainty. Based on the actual geometry, we estimate  $r_g = 6tu/L^2 \simeq 5 \times 10^{-6}$  [4, 19]. In contrast, if we use the measured  $B$  for vacuum and fix  $\phi$  to the established value of  $3.5 - 5 \text{ eV}$  [20], we get values of  $r \simeq 5 \times 10^{-5}$ , one order of magnitude higher than  $r_g$ .

The cause for this discrepancy is likely caused by plastic deformation of the substrate and flow of the polyimide layer in the vicinity of the junction due to inhomogeneous stress [5, 12]. That plastic deformation has to be considered is confirmed by the presence of a residual bending of the substrate after several loading and unloading cy-

cles in some experiments. Moreover, we estimate that a vertical displacement  $z$  of  $\sim 1 \text{ mm}$ , which is a typical excursion needed to break the junction, is sufficient to reach the tensile strength of phosphor bronze. Plastic deformation changes the bending geometry and can substantially lower the mechanical reduction factor, as observed in our experiment.

In addition to the dependence of  $\phi$  on the environment, there is a striking change of the slope  $B$  to smaller values at small  $z$  values, observed in the octane curve ( $\blacktriangleleft$ , Fig. 3(a)) and to a lesser extent in the DCM curve ( $\blacktriangleright$ ). This behavior could be reliably observed for all curves measured in octane after a number of open-close cycles ( $> 30$ ), allowing the junction to stabilize. The observed lowering of the apparent barrier height  $\phi$  is likely caused by the discrete (molecular) nature of the liquid and its behavior in confined geometries [21, 22]. STM investigations have shown that n-alkane chains tend to self-organize parallel to a Au(111) surface [23]. A layering of the octane molecules at short inter-electrodes separations can explain the reduced slope of  $\ln(I)$  vs  $z$  at small gap sizes: for a given vertical displacement  $z$ , the effective shortening of the gap becomes smaller due to the mechanical resistance opposed by the layered octane molecules in between the Au electrodes, deforming the Au extremities. Consequently, a more gentle current increase with vertical displacement results.

In conclusion, we have shown that micro-fabricated break junctions can be operated in a liquid environment opening interesting perspectives to study single-molecule devices in a chemically active environment. We observed that the solvent significantly affects the tunneling regime and obtained good evidence that the confinement of the liquid can lead to molecular layering effects within the gap. We emphasize that the strain limitation of the substrate causes significant variations in the mechanical reduction factor. Despite this difficulty, we could observe a systematic and reproducible trend in the variation of the tunneling barrier height with different solvents.

We are indebted to H. Breitenstein, S. Jakob, P. Reimann and M. Steinacher for technical support. We also thank C. Urbina for kindly hosting one of us (L.G.), and A. Baratoff for helpful discussions. This work benefited from the support of the Swiss National Center of Competence in Research ‘‘Nanoscale Science’’ and the European Science Foundation through the Eurocore’s programme on Self-Organized Nanostructures (SONS).

- 
- [1] A. Nitzan and M.A. Ratner, *Science* **300**, 1384 (2003).  
 [2] N. S. Hush, *Ann. N.Y. Acad. Sci.* **1006**, 1 (2003).  
 [3] J. Moreland, J.W. Ekin, *J. Appl. Phys.* **3888**, 58 (1985).  
 [4] J.M. van Ruitenbeek, A. Alvarez, I. Piñeyro, C. Grahmann, P. Joyez, M.H. Devoret, D. Esteve, C. Urbina, *Rev. Sci. Instrum.* **67**, 108 (1996).  
 [5] N. Agraït, A. Levy Yeyati, J. M. van Ruitenbeek, *Physics Reports* **377**, 81 (2003).  
 [6] M.A. Reed, C. Zhou, C.J. Muller, T.P. Burgin, J.M. Tour, *Science* **278**, 252 (1997).  
 [7] C. Kergueris, J.-P. Bourgoin, S. Palacin, D. Esteve, C. Urbina, M. Magoga, C. Joachim, *Phys. Rev. B* **59**, 12505 (1999).  
 [8] R. H. M. Smit, Y. Noat, C. Untiedt, N.D. Lang, M. van Hemert, J.M. van Ruitenbeek, *Nature* **906**, 419 (2002).  
 [9] J. Reichert, H.B. Weber, M. Mayor, H. V. Löhneysen,

- Appl. Phys. Lett. **82**, 4137 (2003).
- [10] M. Krüger, M.R. Buitelaar, T. Nussbaumer, C. Schönenberger, Appl. Phys. Lett. **78**, 1291 (2001).
- [11] X. Xiao, B. Xu, N. J. Tao, Nano Lett. **4**, 267 (2004).
- [12] S. A. G. Vrouwe, E. van der Giessen, S. J. van der Molen, D. Dulic, M. L. Trouwborst, and B. J. van Wees, preprint.
- [13] E. Scheer, N. Agrait, J.C. Cuevas, A. Levy Yeyati, B. Ludolph, A. Martin-Rodero, G. Rubio Bollinger, J.M. van Ruitenbeek, C. Urbina, Nature **394**, 154 (1998).
- [14] W. Schmickler, Chem. Rev. **96**, 3177 (1996).
- [15] S. M. Lindsay, T. W. Jing, J. Pan, D. Lampner, A. Vaught, J. P. Lewis, O. F. Sankey in *Nanoscale Probes of the Solid/Liquid Interface*, NATO ASI Series E **1993**, Vol 288, 25.
- [16] N. J. Tao, C. Z. Li, H. X. He, J. Electroanal. Chem. **492**, 81 (2000).
- [17] W. Schmickler, D. J. Henderson, J. Electroanal. Chem. **290**, 283 (1990).
- [18] K.L Sebastian, G. Doyen, J. Chem. Phys. **99**, 6677 (1993).
- [19] Calculated using the equations for a simply supported beam. See e.g. W. C. Young, *Roark's Formulas for Stress and strain* (McGraw-Hill, New York, 1989), Chap. 7.
- [20] J. K. Gimzewski, R. Möller, Phys. Rev. B **36**, 1284 (1987).
- [21] B. Bhushan, J. N. Israelachvili, U. Landman, Nature **374**, 607 (1995).
- [22] B. N. J. Persson, F. Mugele, J. Phys.: Condens. Matter **16** R295 (2004).
- [23] A. Marchenko, S. Lukyanets, J. Cousty, Phys. Rev. B **65**, 045414 (2002).